2010 IEEE International Conference on Robotics and Automation
Anchorage Convention District
May 3-8, 2010, Anchorage, Alaska, USA

A New Approach to Time-Optimal Straight-Line Trajectory for Omni-Directional Mobile Robots with Multi-Objective Costs

Ki Bum Kim and Byung Kook Kim, *Member, IEEE*

***Abstract*—We examine time-optimal straight-line trajectory generation for three-wheeled omni-directional mobile robots. Our studies are based on the mobile robot dynamics with battery voltage bounds. We formulate a multi-objective problem that has both translational and rotational costs for time-optimality. Using the switching functions by maximum principle, we present a new approach to determine extreme control components used as motor input. Through the proposed method, we find three combinations of optimal candidates to be the optimal solutions of our problem.**

I. Introduction

Omni-directional mobile robots can move in any direction at any time [1]. Due to their high mobility, omni-directional mobile robots are advantageous for motion in any mission in a tight environment. For example, omni-robots can be used for cleaning, exploration, demining, or reconnaissance.

Time-optimality is considered a fundamental characteristic in any system [2]. In a study of system optimality, it is generally necessary to consider physical constraints as well as the motion equation. In this paper, an accurate dynamic model is used for three-wheeled omni-directional mobile robots (TOMRs) with an orthogonal wheel concept [3]. Also, since electric DC motors are widely used as wheel actuators and the battery voltage is used as the final input to the motors, we consider battery voltage constraints as a practical factor in the time-optimal analysis [4]. Note that, in real-world applications, many path planning strategies based on mobile robot dynamics often produce a combination of simple paths: mostly straight lines and clothoid arcs.

Thus, we consider a time-optimal straight-line trajectory for TOMRs with battery voltage constraints, together with initial and final boundary conditions to take into account translational and rotational costs. Recently, a few researchers have made outstanding contributions to the minimum-time study of TOMR. Near time-optimal analysis aims to decrease computational time to be useful in real-time applications [5], but does not fully reflect the voltage bound and the TOMR dynamics in optimal analysis. Fu *et al.* studied the time-optimality of TOMR with a heuristic algorithm that combined a genetic algorithm and nonlinear programming [6]. However, they did not attempt to avoid computational burden, and did not present the general characteristics for time-optimal motion of TOMR. Balkcom and Mason proposed classification of time-optimal trajectories based on spin in place, circular arc, and singular translation; they also presented an analytic time-optimal study of TOMR over a free path [2]. However, their research is based on kinematics, and it did not address the optimal trajectory required for a specific configuration. In a previous work, we studied time-optimal straight-line trajectory of TOMR without a final heading condition [7]. We remarked on the optimal condition for battery input vector and two optimal candidates for translational and rotational motions. However, that paper focused exclusively on translational cost and excluded rotational cost.

Here we consider not only translational cost but also rotational cost. In other words, our problem will be a multi-objective problem. The core of this problem is how to allocate time to each cost. That is, the switching of optimal candidates is a key issue.

To find a solution to multi-objective problem, we present an analytical method that uses the switching function concept based on maximum principle together with singular cases [8]. Using the proposed method, we find optimal combinations of trajectory types: Trajectory types are extended as the forward and backward motions of optimal candidates. Due to the complexity of TOMR dynamics, we neglect Coriolis terms at the intermediate stage of our analysis. Since Coriolis terms mainly serve to compensate for rapid changes in the TOMR motion, our result can be regarded as reasonable.

II. Dynamics and Problem Statement

A. TOMR Dynamics

The TOMR considered in this paper is equipped with three omni-directional wheel assemblies that are equally spaced at 120-degree intervals, and its radius is l, as shown in Fig. 1.

We represent the TOMR dynamic equations with respect to the coordinated inputs in the base coordinate frame [7]:

$$\ddot{x} = -a\dot{x} - \dot{\phi}\dot{y} + ahu_x \tag{1}$$

$$\ddot{y} = -a\dot{y} + \dot{\phi}\dot{x} + ahu_y \tag{2}$$

$$\ddot{\phi} = -b\dot{\phi} + b(2l)^{-1}hu_\phi \tag{3}$$

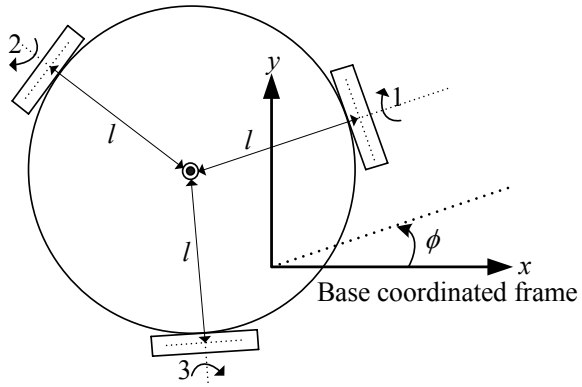

Fig.1. Schematic drawing of TOMR.

where

$$u_x = -\sin\phi u_1 - \sin(\phi + 2\pi/3)u_2 - \sin(\phi - 2\pi/3)u_3 \quad (4)$$

$$u_y = \cos\phi u_1 + \cos(\phi + 2\pi/3)u_2 + \cos(\phi - 2\pi/3)u_3 \quad (5)$$

$$u_\phi = u_1 + u_2 + u_3 \quad (6)$$

a and b are the approximate decay constants of linear and angular TOMR velocities, respectively. The constant h depends on the floor, motor spec, and wheel radius. *We assume that other factors such as nonlinear friction and slip of wheel do not influence on TOMR motion in dynamical situations.* In addition, the coordinated inputs in (4)-(6) are represented by normalized battery voltage inputs $\mathbf{u} = [u_1, u_2, u_3]^T$ to the motor of each wheel.

B. Problem Statement

Allowing TOMR rotation, we analyze the minimum-time straight-line trajectory of TOMR with initial and final heading conditions. As shown in (1)-(3), we pay attention to the Coriolis terms of dynamics by TOMR rotation. We want to determine the minimum-time straight-line solution of TOMR in an arbitrary direction. Without loss of generality, this problem is converted to finding the minimum-time straight-line trajectory with which TOMR moves on the positive x directional straight line, starting with an initial heading angle and stopping with a final heading angle. Since there is no motion in the y direction for the transformed problem, the TOMR dynamics has a constraint of $\dot{y} = 0$ in the entire time interval. In other words, from the y dynamics in (2), we arrive at a constraint on u_y:

$$u_y = -\frac{\dot{\phi}\dot{x}}{ah}, \quad (7)$$

which is required to compensate for the effect of $\dot{\phi}\dot{x}$ in order to maintain $y(t) \equiv 0$.

Thus, we can define the minimum-time straight-line problem for TOMR with the final heading condition as follows:

Problem: Given an initial state $\mathbf{x}(0) = [0,0,\phi_0]^T$, $\dot{\mathbf{x}}(0) = [0,0,0]^T$ and a final state $\mathbf{x}(t_f) = [x_f(>0),0,\phi_f]^T$, $\dot{\mathbf{x}}(t_f) = [0,0,0]^T$ of TOMR, find the minimum time (t_f) subject to the following constraints:

Dynamic constraint: $\ddot{x} = -a\dot{x} + ahu_x$, $\ddot{\phi} = -b\dot{\phi} + b(2l)^{-1}hu_\phi$,

Input constraints: (7) and

$$|u_i| \le 1, \text{ for i = 1, 2, 3.} \quad (8)$$

III. Time-Optimal Analysis

A. Costate Analysis by Maximum Principle

We use the maximum principle to analyze the time-optimality. Initially, we set the costate vector of the state vector $\mathbf{z} = [x, \phi, \dot{x}, \dot{\phi}]^T$ as $\boldsymbol{\lambda} = [\alpha_x, \alpha_\phi, \beta_x, \beta_\phi]^T$. Using the maximum principle, we write the Hamiltonian of our problem with a straight-line constraint as

$$\begin{aligned} H = 1 &+ \alpha_x\dot{x} + \alpha_\phi\dot{\phi} + \beta_x(-a\dot{x} + ahu_x) \\ &+ \beta_\phi(-b\dot{\phi} + b(2l)^{-1}hu_\phi) + p(ahu_y + \dot{\phi}\dot{x}) \end{aligned} \quad (9)$$

Here p is a Lagrangian constant for equality constraint (7).

From $-\dot{\boldsymbol{\lambda}} = \partial H / \partial \mathbf{z}$, costate functions are represented as

$$\alpha_x = \text{negative constant}, \quad (10)$$

$$\dot{\alpha}_\phi = ah(\beta_x u_y - pu_x), \quad (11)$$

$$-\dot{\beta}_x = \alpha_x - a\beta_x + p\dot{\phi}, \quad (12)$$

$$-\dot{\beta}_\phi = \alpha_\phi - b\beta_\phi + p\dot{x}, \quad (13)$$

where $\beta_x u_y$, $p\dot{\phi}$, and $p\dot{x}$ in (11)-(13) are *the by-products stemming from Coriolis terms of the TOMR dynamics*.

Because of the geometric property of input constraints (7) and (8), we find that the optimal condition is when the input vector $\mathbf{u} = [u_1, u_2, u_3]^T$ is at least *2-extreme*, and that two optimal candidates for the coordinated inputs, $\max u_x$ and $\max u_\phi$, are possible for time-optimality of TOMR with rotation [7]. Combining the optimal candidates for overall time remains to be done, before completely resolving the multi-objective problem with both translational and rotational costs. In other words, we can select one of two optimal candidates at any time, but we do not yet consider when to change from one optimal candidate to the other. Thus *the key point to solve our problem is the switching of two optimal candidates*.

To obtain information about the switching of optimal candidates, we investigate the costate functions by the maximum principle. Physically, we consider that the absolute value of α_x and α_ϕ are relevant to x_f and $|\phi_f - \phi_0|$, respectively. Moreover, β_x and β_ϕ are regarded as costate dynamics corresponding to TOMR dynamic equations. Then, what is the physical meaning of p in (11)? We find the answer in Theorem 4.4, which was proved in [7]. The core of Theorem 4.4 is that the nearest wheel of TOMR to the drive-line direction converges to a given straight-line path by $\max u_x$. In other words, when $\max u_x$ is used as the optimal vector, the TOMR heading inevitably changes by extra

rotation i.e., *self-rotation*. This change of heading causes α_ϕ to increase or decrease.

Most notable is that the sign of p is unchangeable and is determined by the initial/final configuration of TOMR. In other words, even if we choose $\max u_x$ as the optimal vector many times, the direction of heading change by $\max u_x$ is preserved for time optimality. Thus we arrive at the following property in addition to the definition remarked in [7].

Definition 1: Considering the time-optimality of the straight-line movement of the TOMR without self-rotation, we find six relative angles to the force direction on the robot motion for maximum translational velocity. These angles are called *the maximum translational angles*, or *MTAs*. Furthermore, three of the six *MTAs*, 0, $2\pi/3$, and $4\pi/3$, are called *stable maximum translational angles*, or *SMTAs*. The other three *MTAs* are called *unstable maximum translational angles*, or *UMTAs*.

Property 1: Consider the time-optimal straight-line problem of TOMR with a battery voltage constraint under the final heading condition. Let α_ϕ be the costate of the TOMR heading. Then, for all initial heading angles other than the *MTAs*, α_ϕ is changed by (11) when the optimal vector with $\max u_x$ is used. Also the sign of the Lagrangian constant p is determined by the heading configuration.

B. Switching Function and Singular Cases

Next we introduce *the switching functions*. Using (4) and (6), the Hamiltonian (9) can be modified as

$$H(\mathbf{u},t) = \varphi_o + \varphi_1 u_1 + \varphi_2 u_2 + \varphi_3 u_3 , \tag{14}$$

where $\varphi_o = 1-(\dot{\beta}_x + p\dot{\phi})\dot{x} - (\dot{\beta}_\phi + p\dot{x})\dot{\phi}$ and

$$\begin{pmatrix}\varphi_1\\ \varphi_2\\ \varphi_3\end{pmatrix} = ah\begin{pmatrix} -\beta_x \sin\phi + b(2la)^{-1}\beta_\phi \\ -\beta_x \sin(\phi + 2\pi/3) + b(2la)^{-1}\beta_\phi \\ -\beta_x \sin(\phi - 2\pi/3) + b(2la)^{-1}\beta_\phi \end{pmatrix}. \tag{15}$$

φ_i is considered to be *the switching function*. In time-optimal analysis with a constant bounded input domain, the switching function is very useful to determine the extreme inputs [8]. Decision rule of the extreme input is as follows.

$$u_i = \begin{cases} 1 & if\ \varphi_i < 0 \\ -1 & if\ \varphi_i > 0 \\ undefined & if\ \varphi_i = 0 \end{cases} \tag{16}$$

Of course, by the optimality condition, one non-extreme input is constrained by straight-line motion and two extreme inputs are determined from (16) when $\max u_x$ is used.

At this point, it is necessary to take the case when $\varphi_i = 0$ into account. If any switching function remains at zero, then two cases are possible: one is that $\varphi_i = 0$ happens instantaneously, the other is that $\varphi_i = 0$ is maintained for a nontrivial time interval. The former means that there is a change among extreme input components, and it is a necessary condition for the switching of optimal candidates. However, the meaning of the latter is somewhat different. If any switching function remains at zero for a non-zero time interval, then switching control happens at the boundary of the time interval. This control can be regarded as the exceptional case.

Conventionally, we call 'u_i singular' when the switching function φ_i is identically zero during a nontrivial time interval [8]. When the switching problem is handled, considering the singular case is often very important. In our problem, we know that *the singular case only happens when TOMR with* $\max u_x$ *moves in any MTA line*; the non-extreme input component is always zero. Therefore, we should consider all singular cases in our analysis.

Finally, we connect switching functions with costate functions. For this, we define *Level K* as follows:

$$K = -\frac{b}{2la}\frac{\beta_\phi}{|\beta_x|} \tag{17}$$

Then, we rewrite (15) for u_i switching functions as

$$[\varphi_1, \varphi_2, \varphi_3]^T = -\mathrm{sgn}(\beta_x)ah\,|\beta_x| \cdot ([\zeta_1, \zeta_2, \zeta_3]^T - K), \tag{18}$$

where $\zeta_i = \sin(\phi + 2(i-1)\pi/3)$.

As shown in (17)-(18), the switching function is at large composed of two elements: one is composed of sine functions with respect to the current TOMR heading; the other is *Level K,* which depends on the costate functions by the maximum principle. If the change in the *Level K* is known, then we can determine the extreme input vector from (16) at any time.

However, we cannot obtain the explicit form of the costate function because of the complexity of TOMR dynamics by the Coriolis terms. Nevertheless, to gain insight into the switching of optimal candidates, it is meaningful to analyze our problem based on TOMR dynamics *excluding Coriolis terms*.

C. Case Study (Without Final Velocity Constraints)

As a preliminary step, we *release the boundary condition for the final velocity*. When the final velocity conditions are free, β_x and β_ϕ at the final time are both zero. From (11)-(13), we can represent the costate functions as

$$\beta_x = \alpha_x a^{-1}(1-e^{a(t-t_f)}),\ \beta_\phi = \alpha_\phi b^{-1}(1-e^{b(t-t_f)}),\ \dot{\alpha}_\phi = -pahu_x .$$

Then, *Level K* in (17) is rewritten as

$$K = \frac{-\alpha_\phi}{2l\,|\alpha_x|} w(t), \quad for\ t \in [0,\ t_f) \tag{19}$$

where

$$w(t) = (1-e^{b(t-t_f)})(1-e^{a(t-t_f)})^{-1}. \tag{20}$$

As shown in (19)-(20), since a, b, and α_x are all constants, the change in *Level K* depends on $w(t)$ and α_ϕ. Concretely, since α_ϕ is unchanged with the use of $\max u_\phi$, *Level K* depends on $w(t)$ only. On the other hand, if $\max u_x$ is used, the change of α_ϕ is considered for the estimation of *Level K*. In summary, we arrive at the following *Level K* property.

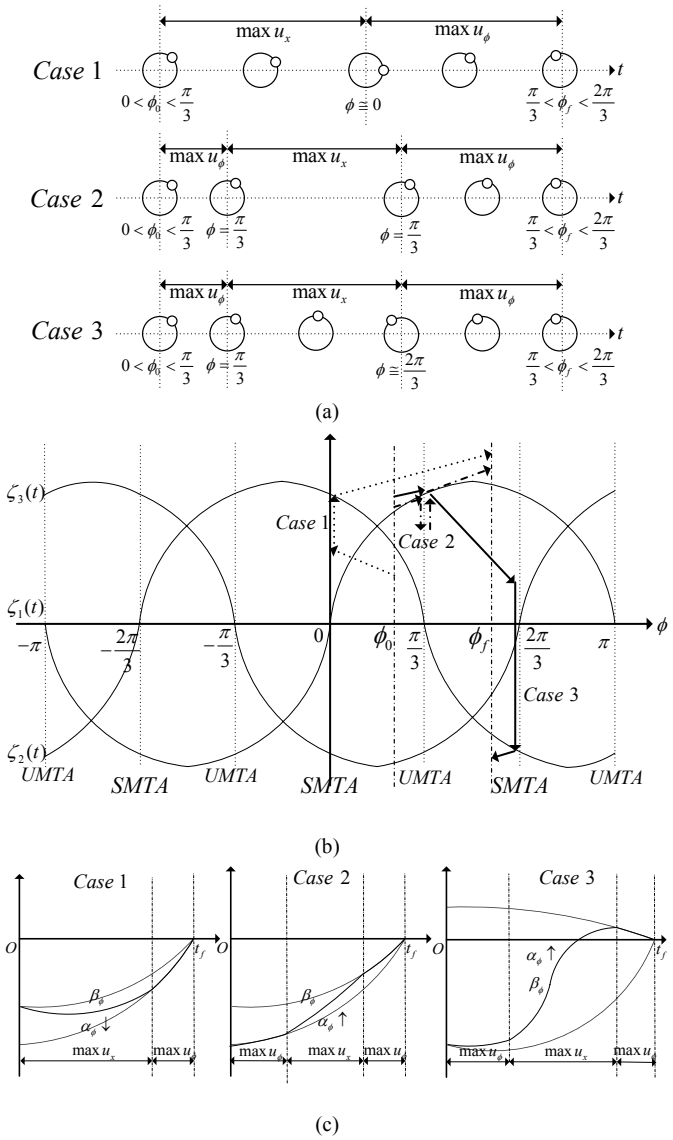

Fig. 2. Analysis of example with *K-graph*. (a) Three ways for the motion of TOMR are shown when the initial/final conditions in the example are $0 < \phi_0 < \pi/3$ and $\pi/3 < \phi_f < 2\pi/3$; TOMR uses zero degrees *SMTA* in Case 1, 60 degrees *UMTA* in Case 2, and 120 degrees *SMTA* in Case 3. (b) The expected trace of *Level K* in the *K-graph* for each case. (c) The plot of β_ϕ by the change of α_ϕ for each case.

Property 2 (The property of Level K): Consider the time-optimal straight-line trajectory of TOMR with a battery voltage constraint under the final heading conditions. Assume that the TOMR dynamics has *no Coriolis terms.* Then, *Level K* defined as (19) is a *continuously differentiable* function, and $w(t)$ is an *increasing* function with respect to time.

Since $w(t)$ and α_ϕ are continuously differentiable, it is obvious that *Level K* in Property 2 is continuously differentiable. Also, using the mean value theorem, we can show that $w(t)$ is an increasing function with respect to time.

Now we investigate how *Level K* changes. We focus on the change of *Level K* in the ϕ domain. For this, we propose the graph as shown in Fig. 2(b), and call it a *K-graph*. Horizontal axis in the *K-graph* is the TOMR heading ϕ. The extreme inputs at any time are determined by (16) thorough the trace of *Level K* in *K-graph* with ζ_i s.

Also, based on the position of *Level K* in the *K-graph*, we know which optimal vector should be chosen. We define the ζ *envelope* as the outermost boundary set of ζ_i s in the *K-graph*. If the *Level K* is located *inside the* ζ *envelope*, then the optimal vector is $\max u_x$. Conversely, if *Level K* is located *outside the* ζ *envelope*, then the optimal vector is $\max u_\phi$. Thus the switching of optimal vectors happens when the *Level K* intersects with the ζ *envelope*.

Let us consider an example with a *K-graph*. Initial and final heading conditions of the example are seen in Fig. 2(a). Basically, α_x is a negative constant because $x_f > 0$. Thus, β_x is always negative for $t \in [0, t_f)$. In the same manner, the sign of $\alpha_\phi(t)$ depends on the remaining rotation to the final heading at any time. Thus $\alpha_\phi(0)$ is negative in the example, in turn, *Level K* at the initial time is positive.

As shown in Case 1 in Fig. 2(b), we assume that *Level K* starts with any positive value inside the ζ *envelope* at ϕ_0. Then the TOMR heading changes to the nearest wheel (zero degree line) according to Theorem 4.4 [7]; as a result, $\alpha_\phi(t)$ decreases. At the same time, the absolute value of *Level K* may be influenced by the change of $\alpha_\phi(t)$. As time goes by, the absolute value of *Level K* increases according to Property 2, and then it escapes from the ζ *envelope*; otherwise, the final heading condition is never satisfied. Moreover, once *Level K* is outside the ζ *envelope*, the optimal vector is switched to $\max u_\phi$, and the absolute value of *Level K* increases according to Property 2, so the *Level K* can never reenter the ζ *envelope* for $0 < \phi < \pi/3$. In Case 1 in the example, the switching of optimal vectors occurs only one time: $\max u_x$ followed by $\max u_\phi$. Moreover, the approximate β_x and β_ϕ are shown in Fig. 2(c).

Next we assume that the *Level K* at ϕ_0 is initially located outside the ζ *envelope*. In Case 2 in Fig. 2, the initial rotation is used so that the TOMR heading is exactly 60 degrees. After that, TOMR has translational motion on the *UMTA*; this is clearly the singular case. During the translational motion by $\max u_x$, the *Level K* initially decreases by $\alpha_\phi(t)$, and then it increases by $w(t)$. Finally, if the *Level K* escapes from the ζ *envelope,* then TOMR rotates to ϕ_f.

Likewise, we can make another choice for the trace of *Level K* that is relevant to singular case. If the TOMR heading crosses the 60 degrees *UMTA* by initial rotation, then the remaining angle gap before the final rotation is about $\phi_f - 2\pi/3$. Thus Case 3 in Fig. 2(b) can be a trace of *Level K* in relation to the singular case.

Through Cases 2 and 3, we investigated two ways to connect singular case with the trace of *Level K* in *K-graph*:

one is to place the TOMR heading on the nearest *UMTA*; the other is to cross the TOMR heading over to the next *SMTA*.

D. Number of Switchings and Optimal Trajectories

In subsection C, we investigated the switching of optimal candidates without final velocity conditions through the example. However, we have not yet investigated how many additional switchings are needed. For this, we try to capture characteristics for the trace of *Level K* in the *K-graph*. In particular, we consider how the trace of *Level K* changes in the *K-graph* after switching from $\max u_x$ to $\max u_\phi$. Without loss of generality, we assume that $-\pi/6 < \phi_0 < \pi/2$ and $\phi_f > \pi/2$. Let us consider several situations in the *K-graph,* as shown in Fig. 3.

If *Level K* escapes from ζ_2 in the *ζ envelope* at $-\pi/6 < \phi < \pi/6$ as shown in cases I and II in Fig. 3, *Level K* never enters inside an upper part of ζ_2 by Property 2. As shown in case III of Fig. 3, if *Level K* encounters ζ_1 at a smaller heading angle than $\pi/3$ and the optimal vector changes to $\max u_x$, the absolute value of α_ϕ increases according to Theorem 4.4 [7] because the difference between the current heading angle and the final heading is larger. Thus, this case can never happen because the absolute value of *Level K* cannot decrease. In cases IV and V, switching to $\max u_x$ happens at a more than $\pi/3$. These cases are involved with the singular case, like Cases 2 and 3 of the example in subsection C.

Finally, it is necessary to check the possibility of the trace of *Level K* as the case VI in Fig. 3. If *Level K* escapes from the *ζ envelope* at $0 < \phi < \pi/3$ and enters the *ζ envelope* at $\pi/3$, then the sign of the time derivative of α_ϕ in preceding $\max u_x$ (before escaping from the *ζ envelope*) is different than that in following $\max u_x$ (after reentering the *ζ envelope*). This is contradictory to Property 1, so case VI cannot occur in an optimal trajectory.

From cases I to VI, we can infer the following facts: first, *if* $\max u_x$ *is chosen as the first optimal vector, the optimal vector is just switched to* $\max u_\phi$ *one time to meet the final heading*, i.e. more than two switchings do not happen; second, *if* $\max u_\phi$ *is chosen as the first optimal vector, additional switching is required to switch to* $\max u_x$ *at near UMTA*, after then, just one switching to $\max u_\phi$ is necessary for the final heading conditions.

When we consider the original problem presented in Section II, deceleration (breaking) procedure as well as acceleration phase for translational and rotational motions are additionally required to meet the final velocity conditions, as shown in Fig. 4(a). In a similar manner to subsection C, we can draw the trace of *Level K* in the *K-graph,* as shown in Fig. 4(b). Fig. 4 shows an example of the trace of *Level K* that is not related to the singular case.

Before we summarize our work, for convenience, we divide optimal candidates into detailed trajectory types.

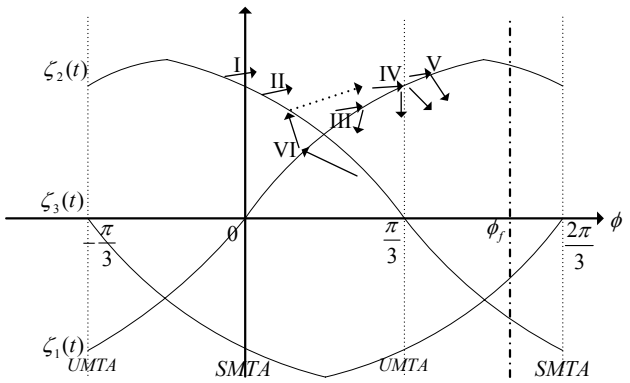

Fig. 3. Several cases of the switching of optimal vectors in the *K-graph.*

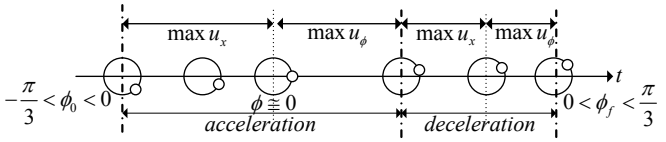

(a)

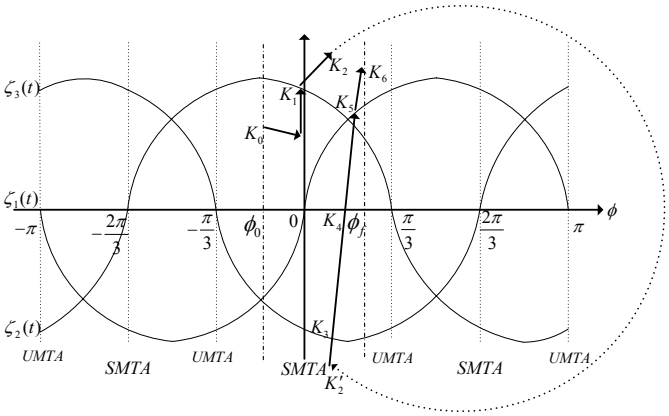

(b)

Fig. 4. An example of the trace of *Level K* with final velocity constraints in the *K-graph.* (a) Initial and final conditions in the example are $-\pi/3 < \phi_0 < 0$ and $0 < \phi_f < \pi/3$; TOMR uses zero degrees *SMTA*. (b) The expected trace of *Level K* in *K-graph*; *Level K* starts from K_0 at ϕ_0 and arrives in K_6 at ϕ_f; Two switchings to $\max u_\phi$ happen at K_1, K_5 and one switching to $\max u_x$ occurs at K_3; The sign of the costate functions, β_x and β_ϕ, changes at K_2, K_4.

Definition 2: Define T^+, T^-, R^+, R^- as four different trajectory types. The letters T, R represent the TOMR motion by optimal vector, $\max u_x$ and $\max u_\phi$, respectively. Also, the superscripts $+, -$ indicate whether the direction of motion is forward or backward. Additionally, R_o^+, R_o^- with the subscript o mean the initial rotations.

In particular, the meaning of "forward" in rotational operation depends on the amount of remaining rotation toward the final heading when $\max u_\phi$ is selected; if $\phi > \phi_f$, then clockwise rotation is forward, otherwise, counterclockwise is forward.

In conclusion, considering backward motion, we present the following property for the optimal trajectory.

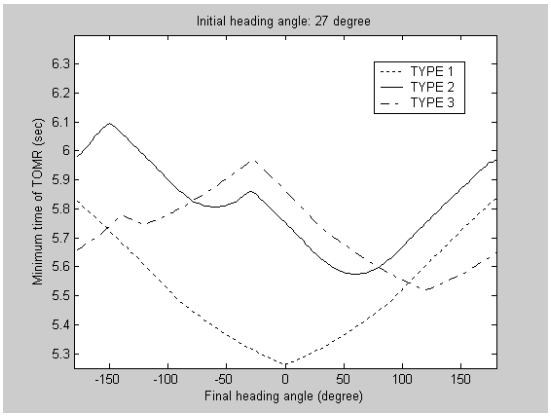

(a)

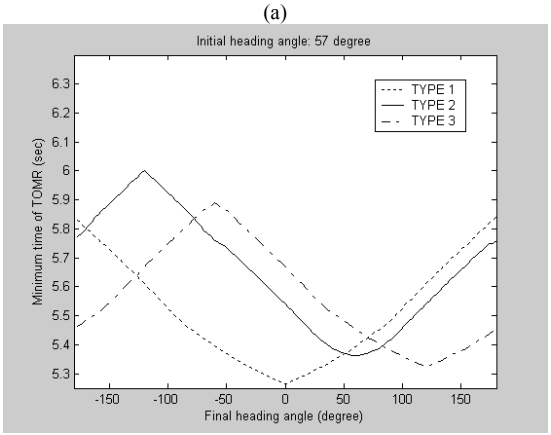

(b)

Fig. 5. Comparison of each combination of trajectory types in $0 < \phi_f < 180^\circ$ and (a) $\phi_0 = 27^\circ$ (b) $\phi_0 = 57^\circ$; TYPE 1 ($T^+R^+T^-R^-$) , TYPE 2 ($R_o^+R_o^-T^+R^+T^-R^-$), TYPE 3 ($R_o^+T^+R^+T^-R^-$).

Property 3 (Optimal trajectories): When we consider the problem presented in Section II, the *optimal trajectory is one among the following three concatenations of trajectory types:* $T^+R^+T^-R^-$, $R_o^+R_o^-T^+R^+T^-R^-$, and $R_o^+T^+R^+T^-R^-$.

IV. Simulation

In this section, we perform a simulation to compare three combinations of trajectory types according to various configurations. In particular, although the proposed method with *Level K* in the *K-graph* neglected Coriolis terms, we use TOMR dynamics *with* Coriolis terms in our simulation in order to verify the validity of the derived properties. In the simulation, we set the straight-line length of the TOMR to be 5 m, the time resolution as 1 ms, and the maximum error criterion for stopping the simulation as less than 0.1%. In addition, the TOMR parameters are $a = 2.8368$, $b = 6.1953$, $l = 0.188$, and $h = 0.6024$.

To investigate the general trend among each combination of trajectory types, we assume two fixed initial heading angles in Fig. 5. For all final heading angles, $R_o^+R_o^-T^+R^+T^-R^-$ (Type 2) can never be the optimal combination of trajectory types at $\phi_0 = 27^\circ$, as shown in Fig. 5(a). However, $R_o^+R_o^-T^+R^+T^-R^-$ (Type 2) can be the optimal combination for some final heading angles around 60° as Fig. 5(b). From these results, we can expect that Type 2 can be an optimal combination when ϕ_0 and ϕ_f are located near the *UMTA*. Also, as shown in Fig. 5, the huge gap between the initial heading and final heading shows that there is a higher chance that $R_o^+T^+R^+T^-R^-$ (Type 3) is optimal.

V. Conclusion

This paper focuses on the time-optimal straight-line trajectory for TOMRs. It is distinct from other works because we use the TOMR dynamics with Coriolis terms and also battery voltage constraints as a platform of our studies. In addition, the problem defined in this paper is a multi-objective problem, which has both translational and rotational costs. To handle the muti-objective costs, we present a new approach that uses the switching function concept with singular cases. In particular, we introduce *Level K* and *K-graph* for the analysis.

We do not yet consider the time-optimal trajectory with non-straight paths, such as a circular arc or a combination of circular arcs and straight lines. In the near future, our research will be extended to the time-optimal problem with any paths.

Acknowledgement

This work was supported (in part) by Ministry of Knowledge Economy under Human Resources Development Program for Convergence Robot Specialists.

References

[1] F. G. Pin and S. M. Killough, "A New Family of Omnidirectional and Holonomic Wheeled Platform for Mobile Robots," *IEEE Trans. Robotics and Automation,* vol. 10, no. 4, pp. 480-489, 1994.

[2] D. J. Balkcom, P. A. Kavathekar, and M. T. Mason, "Time-Optimal Trajectories for an Omni-Directional Vehicle," *Int. J. Robotics Research,* vol. 25, no. 10, pp. 985-999, 2006.

[3] K. Watanabe, "Control of an Omnidirectional Mobile Robot," *Proc. of the 2nd KES Int. Conf. Knowledge-Based Intelligent Electronic Systems*, vol. 1, pp. 51-60, 1998.

[4] J. S. Choi and B. K. Kim, "Near-Time-Optimal Trajectory Planning for Wheeled Mobile Robots with Translational and Rotational Sections," *IEEE Trans. Robotics and Automation,* vol. 17, no. 1, pp. 85-90, 2001.

[5] T. Kalmar-Nagy, R. D'Andrea, and P. Ganguly, "Near-Optimal Dynamic Trajectory Generation and Control of an Omnidirectional Vehicle," *Robotics and Autonomous Systems,* vol. 46, no. 1, pp. 47-64, 2004.

[6] Y. Y. Fu, C. N. Ko, T. L. Lee, and C. J. Wu, "A Nonlinear Programming Method for Time-Optimal Control of an Omni-Directional Mobile Robot," *J. Vibration and Control,* vol. 14, no. 11, pp. 1729-1747, 2008.

[7] K. B. Kim and B. K. Kim, "Minimum-Time Straight-Line Trajectory for Three-Wheeled Omni-Directional Mobile Robots with Voltage Constraint," *39th Int. Symposium on Robotics,* vol. 1, pp. 755-760, 2008.

[8] H. J. Sussmann and G. Tang, "Shortest Paths for Reeds-Shepp Car: A Worked out Example of the Use of Geometric Techniques in Nonlinear Optimal Control," Rutgers Center for System and Control Report 91-10, 1991.